SPIE's International Symposium on Interferometry in Space – Waikoloa, Hawaii USA – vol. 4852 – August 2002

Alignment of the MAM testbed to enable micro-arcsecond astrometry performance for SIM.

Renaud Goullioud[1], Eric Bloemhof
Jet Propulsion Laboratory, California Institute of Technology

ABSTRACT

Future space-based optical interferometers, such as the Space Interferometer Mission, require fringe measurements to the level of picometers in order to produce astrometric data at the micro-arc-second level. To be more specific, it is necessary to measure both the position of the starlight central fringe and the change in the internal optical path of the interferometer to a few tens of picometers. The internal path is measured with a small metrology beam whereas the starlight fringe position is estimated with a CCD sampling a large concentric annular beam. One major challenge for SIM is to align the metrology beam with the starlight beam to keep the consistency between these two sensors.

The Micro-Arcsecond Metrology testbed (MAM) developed at the Jet Propulsion Laboratory features an optical interferometer with a white light source, all major optical components of a stellar interferometer and heterodyne metrology sensors. The setup is installed inside a large vacuum chamber in order to mitigate the atmospheric and thermal disturbances. Both the white light and metrology sensors have been proven to work independently at the required levels. The next step is to integrate them together as a micro-arc-second capable system. A complex alignment sequence has been developed in order to match the absolute tilt and shear of the metrology and starlight paths to 1 micro-radian and 10 micrometers respectively. This paper describes the MAM optical setup, the alignment process, the contribution of the fine alignment to the final performance and how they relate to SIM.

Keywords: Interferometry, SIM, metrology, alignment.

1. INTRODUCTION

The MAM experiment is a key ground-based testbed that will demonstrate some critical technologies for SIM, the Space Interferometry Mission. SIM is discussed in more detail elsewhere in this volume[1], but is in essence a space-based Michelson interferometer that will carry out astrometry to micro-arcsecond precision on the visible light from a large sample of stars in our galaxy. Interferometry of such high precision requires extremely accurate knowledge of interferometer baselines, and hence extremely precise internal metrology, which is to be carried out with near-infrared laser heterodyne metrology gauges working at the 1319 nm wavelength of Nd:YAG. For SIM to succeed, the optical path-length metric provided by the interferometer fringe determination must be faithfully tracked to the level of tens of picometers by the distances measured by metrology gauges, through all the operational motions of interferometer delay line and siderostats. The purpose of MAM is to demonstrate this agreement in a large-scale simulation that implements a substantial fraction of the final SIM flight baseline.

Figure 1 is a picture of the MAM experiment in the chamber that provides the vacuum necessary to obtain the sub-nanometer performance. The MAM naturally divides into two distinct subsystems: the Test Article (TA), which is the interferometer proper, and the Inverse Interferometer Pseudo-Star (IIPS), which emulates a distant star under observation by providing spatially coherent wavefronts out of two mirrors, separated by the MAM baseline, that feed directly into the two siderostats of TA. The spectrum of the 600-1000 nm white light ("starlight") generated by IIPS corresponds to that of a blackbody at a temperature of about 3100 K. A schematic optical layout of MAM is shown in Figure 2. In addition to the central main beam combiner, which is the beam splitter at which light from the two arms of the interferometer are combined to produce interference, TA contains a CCD camera to record fringes, a delay line to adjust the OPD between the two arms of the interferometer to the desired value, and a voice-coil modulator (VCM) to scan the OPD for fringe fitting. In addition to the white light source, IIPS contains a number of auxiliary light sources at different wavelengths that are used as beacons for alignment of system optics; one auxiliary light source provides an alternative metrology test (full aperture metrology, or

[1] Send correspondence to: renaud@jpl.nasa.gov; m/s 171-113, 4800 Oak Grove Dr, Pasadena, CA91109;
Phone: 818 354 7908

FAM). Some of the technical details of MAM are discussed elsewhere in this volume[2], and some will be described more fully in later sections.

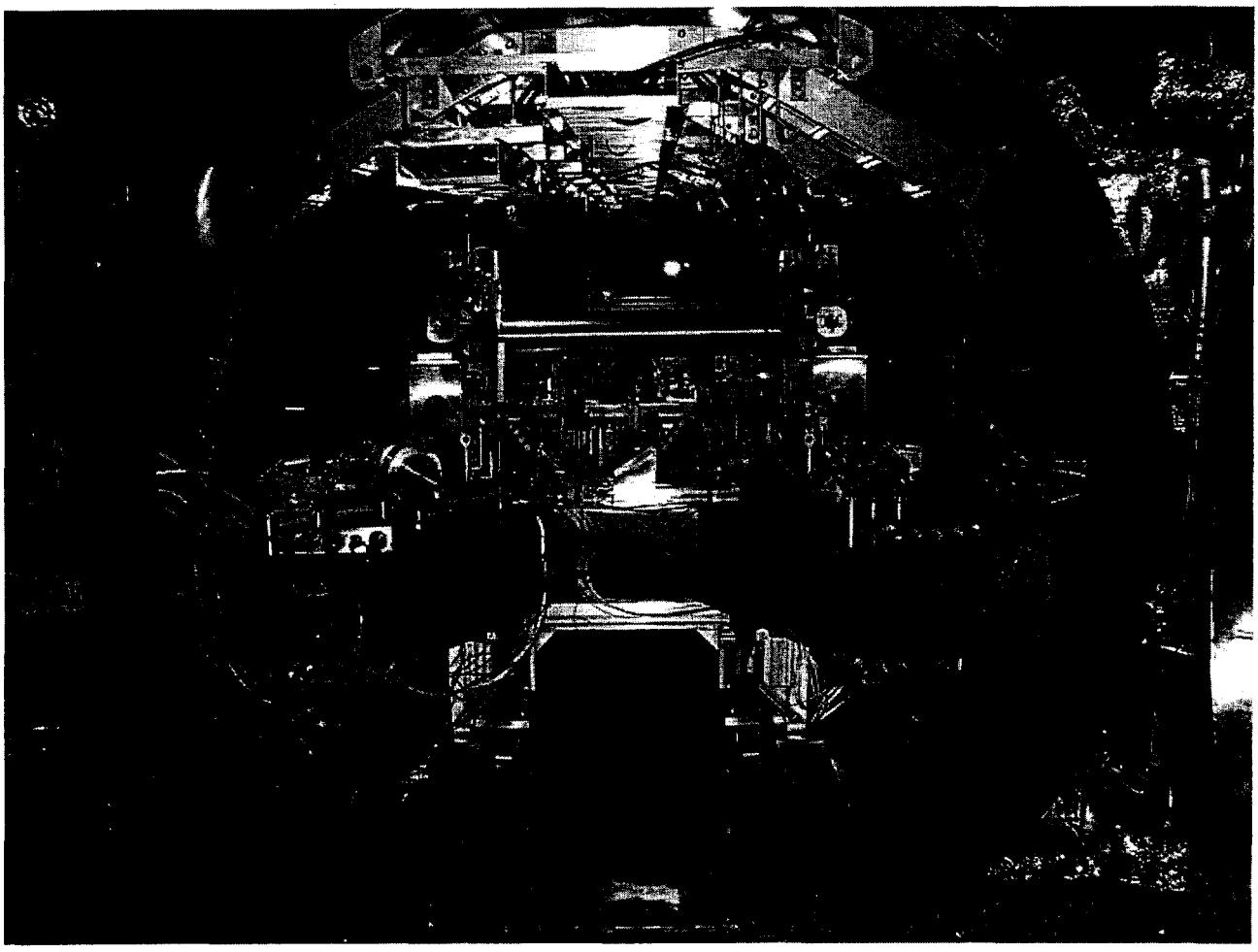

Figure 1: The MAM experiment in the 45 foot long vacuum chamber.

A severe technical constraint on the problem of tracking interferometry with metrology to picometer precision is faced by MAM as it will be by SIM: the white light signal measured by the interferometer travels in an annular beam that fills most of the 40 cm siderostats, while the 1319 nm laser light for metrology travels in pencil beams located within the "sub-aperture", or obscured 18 cm center of these annuli, where they are directed to small reference corner cubes at the centers of the siderostats. The very different optical footprints of interferometry and metrology beams puts a premium on accurate optical alignment, which has led to the development of the techniques discussed in this paper.

2. THE MAM DESIGN IN MORE DETAIL

More precisely, the conceptual dividing line between TA, the interferometer, and IIPS, the light source that emulates spatially coherent light from a distant star, is at the vertices of the two small corner cubes that are located within the sub-apertures of the two siderostats in TA. As part of the alignment procedure, the vertices are arranged to be precisely coincident with the rotation axes of the siderostats. Metrology gauge launchers in both TA and IIPS measure round-trip distances, with precision in the neighborhood of 10 pm, to and from the vertices of these corner cubes; for this reason, the launcher in this scheme is designated SAVV, for Sub-Aperture Vertex-to-Vertex. Reference[5] presents details and stand-alone performance of the SAVV metrology launcher. Placing the vertices on the siderostat rotation axes is clearly a first step to maintaining agreement between white-light and metrology OPD as the siderostats are moved to carry out "field dependent" tests that simulate observations of multiple stars with SIM.

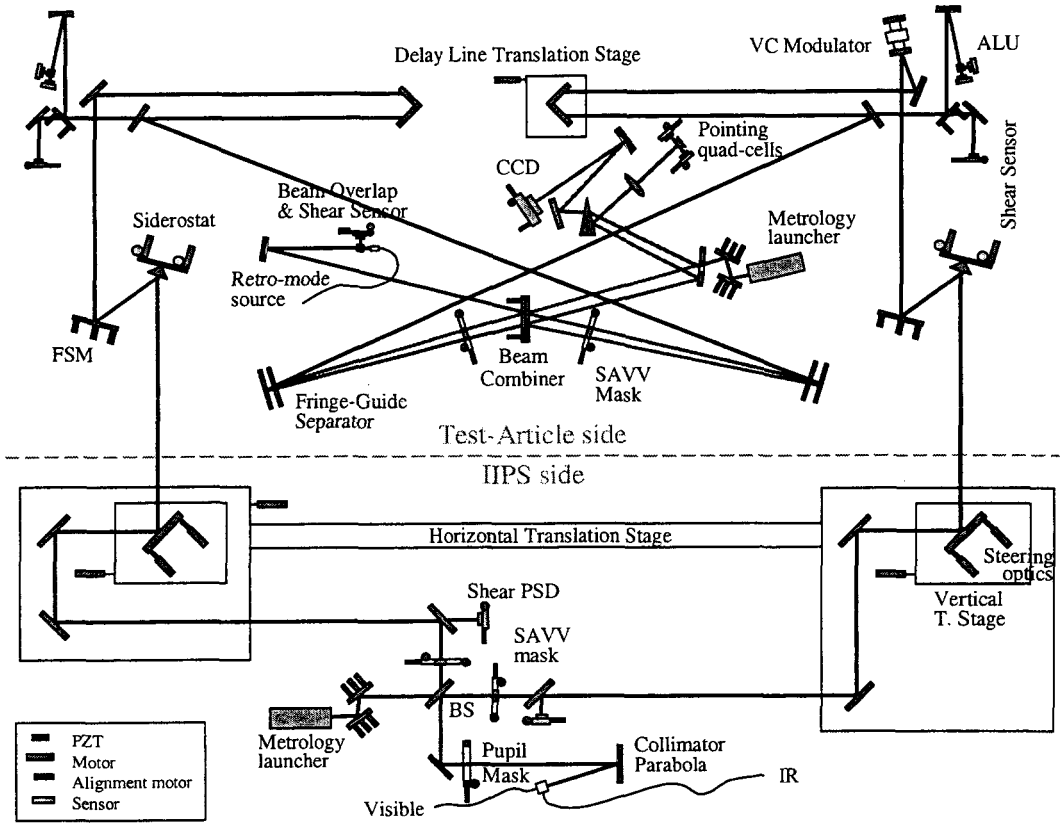

Figure 2: MAM main optical layout.

There is one difference between TA and IIPS regarding how the metrology beams are handled. The "metrology launchers" on each subsystem are capable of launching and receiving 1319 nm metrology light, but on the IIPS side metrology light may also be introduced via the cube beam splitter near the very bottom of Figure 2. There, white "starlight" and the various auxiliary beacons and FAM are introduced on the fiber labeled "Visible", to be combined with 1319 nm metrology radiation introduced on the fiber labeled "IR". Launching white-light and metrology light from a single source in this way permits co-alignment of the beams to high accuracy. This separation of metrology beam launch from metrology reception and heterodyne detection, which still occur in the "metrology launcher" box, is termed "split-SAVV" mode.

The white-light and metrology beams emerge from the cube beam splitter in IIPS with beam patterns typical of launching into free space from bare fibers, ~f/8 or so, and they are collimated by an off-axis paraboloid (Figure 2) before being directed to the main beam splitter (BS) that will divide the beams for the two output arms of IIPS. A set of two compensating beam splitters, with substrates and coatings identical to those of the main beam splitter, maintains uniformity between the two arms by ensuring that each path experiences both a transmission and a reflection. A "pupil" mask defines the annular beam for white-light. "SAVV" masks, different in each arm of IIPS, define the sub-aperture metrology beams; these are configured as sets of two square pencil beams in the inner part of the annulus, with the pencils stacked vertically in one arm and horizontally in the other arm of IIPS. The output beams, the outer, annular ("full-aperture") white-light beam with inner, "sub-aperture" pencil beams of 1319 nm metrology light, are sent from two IIPS steering mirrors directly opposite TA's two siderostats. To accommodate motions of the siderostats that emulate observations of multiple target stars, the IIPS steering mirrors are mounted on translation stages whose motions are determined as part of the alignment procedure.

The white-light beam, before injection into the cube beam splitter for combination with metrology light, has been combined with laser beacons, at 532, 633, and 980 nm, that are used in the alignment procedure. Also available is a full-aperture metrology (FAM) signal, an annular beam at 660 nm that is obtained by doubling from the source that delivers 1319 nm light for metrology. Optimum performance of IIPS, which has very stringent requirements on wavefront quality over one output beam (~$\lambda/4$) and uniformity between the two arms ($\lambda/10$), requires accurate co-alignment of white-light and metrology beams in both tip/tilt and shear. Shear detectors ("Shear PSD" in Figure 2), mounted behind the compensating beam splitters, will be used for this determination.

At the TA siderostats, the white-light signal passes through for fringe measurement by TA, the interferometer proper. The metrology light originating in IIPS is retro-reflected and retraces its path through the IIPS optics until it is returned to the metrology box shown in Figure 2 for heterodyne detection. A corresponding pair of sub-aperture metrology beams originates in the metrology launcher in TA, and measures the round-trip distances along the two arms of the interferometer between the launcher and the same corner-cube vertices. In this way the complete optical path traversed by white-light is measured by metrology, in two pieces. The siderostats control gross pointing, but they are fed by fast-steering mirrors (FSM), which carry out high-bandwidth tip-tilt corrections to lock the peak of the white-light signal onto a certain point on the CCD. The FSM control loops are closed with a signal derived from the blue portion of the white-light beam, which is diverted by the "fringe-guide separators" in Figure 2 and directed into the "pointing quad-cells". Figure 2 shows an auxiliary light injection source on TA, the "retro-mode source", that is not used in standard operation of the testbed, but permits preliminary tests of TA operation without the IIPS pseudo star. In this mode, the light injected by the retro-mode source traverses the optics of TA in a roundtrip, to and from a pair of special corner cubes positioned in front of the siderostats.

3. REQUIREMENTS

The challenge of the MAM experiment is to measure the same path using two separate and quite different optical probes. The heterodyne metrology gauge uses a compact, bright and highly coherent laser beam. Therefore, one can expect high resolution measurements. The starlight sensor collects a larger, weaker beam from a faint, incoherent source (a nearby star for SIM, or a light bulb coupled to a fiber for MAM). To maximize the amount of collected star light, the sub-aperture metrology beam must be as compact as possible. The two beams are concentric, but they do not overlap. Also, to avoid cross-contamination of the two light beams, metrology is carried out at a much different wavelength (1.3 μm) than is used for starlight observations (the 0.6 to 1.0 μm band). The metrology beam uses the central portion of the optics and retro-reflects on the corner-cube, so as to travel a roundtrip through the MAM optics. The starlight reflects on the annular portion of the optics and travels only once through the optical train. Finally, the pathlength estimation from the heterodyne metrology sensor and the dispersed fringe sensor will have different errors specific to these very different techniques.

In summary, there are many known reasons why infrared metrology and white light interferometry will disagree. The wavelength difference will cause dispersion-related errors that are very sensitive to thermal effects. Diffraction effects will be quite different for metrology and starlight, an issue that is addressed in the diffraction testbed experiment.[4] Beam walk on the optics will cause errors due to imperfect wavefront quality: even an optic figured to 1/100 of a wave RMS has surface irregularities of 6000 pm rms. As the small metrology beam moves around, or "walks", on this surface, the path length difference between metrology and starlight is going to change[3]. In the current study, we are addressing one of the potentially largest sources of error in MAM: imperfect geometric alignment between the metrology and starlight beams.

The starlight beam is emitted by the star, collected by the siderostats and detected in the spectrometer. The metrology beam is issued by the launcher, retro-reflected on the corner-cube and detected back in the launcher. Where the metrology and the starlight beams share the same optics, they have to measure the pathlength with a few picometers accuracy. Even with the best effort, the two concentric beams are not fully concentric, indeed they will be offset laterally by a distance S (shear). The two beams will be approximately parallel, with a small residual tilt φ. At the recombination (see Figure 3), the two beams will have traveled to the first order the same path with a slight difference $d = S \cdot \varphi$. If φ is only 10 micro-radians (or 2 arc-seconds) and S is only 100 microns, the pathlength difference is already 10 μrad · 100 μm = 1000 pm (picometers).

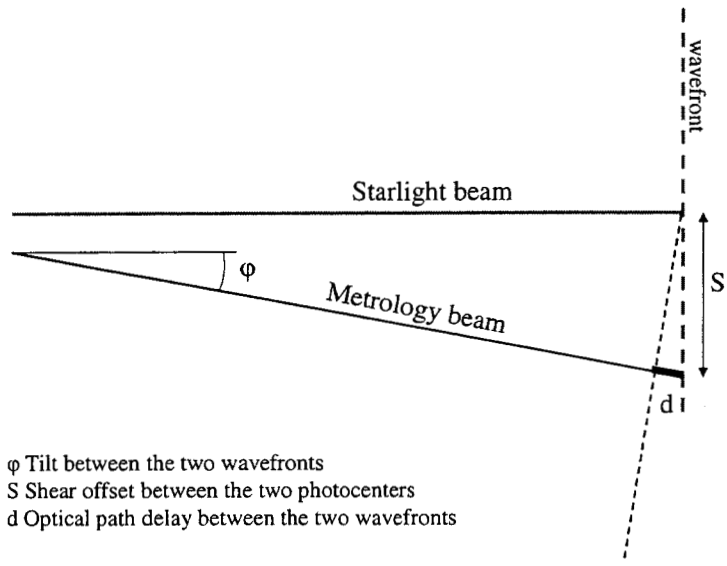

Figure 3: Pathlength error due to misalignment between the metrology beam and the starlight

However the metrology is only a relative sensor tracking the changes in optical path. Therefore, an absolute delay of a few hundreds of picometers over meters of optical path is not an issue. The real issue is changes on the delay. If the tilt changes by $\Delta\varphi$, the delay between the metrology and the starlight paths will be $\Delta d = S \cdot \Delta\varphi$. Reciprocally, a slight shear of the metrology beam relative to the starlight beam by ΔS will cause an error in the path measurement $\Delta d = \varphi \cdot \Delta S$. One will notice that if the absolute tilt between the metrology and the starlight wavefront φ is small to start with, the sensitivity to shear jitter and drift ΔS is small. Similarly, if the absolute shear between the two concentric beams S is small, the sensitivity to the tilt jitter and drift $\Delta\varphi$ is smaller too. Therefore, it is critical to optimize the absolute tilt and overlap alignment between the metrology and the starlight beams. Figure 4 shows how the allocated error for MAM has been divided between the various sub-systems. In particular, 20pm are allocated the relative alignment between the metrology and the star light beams.

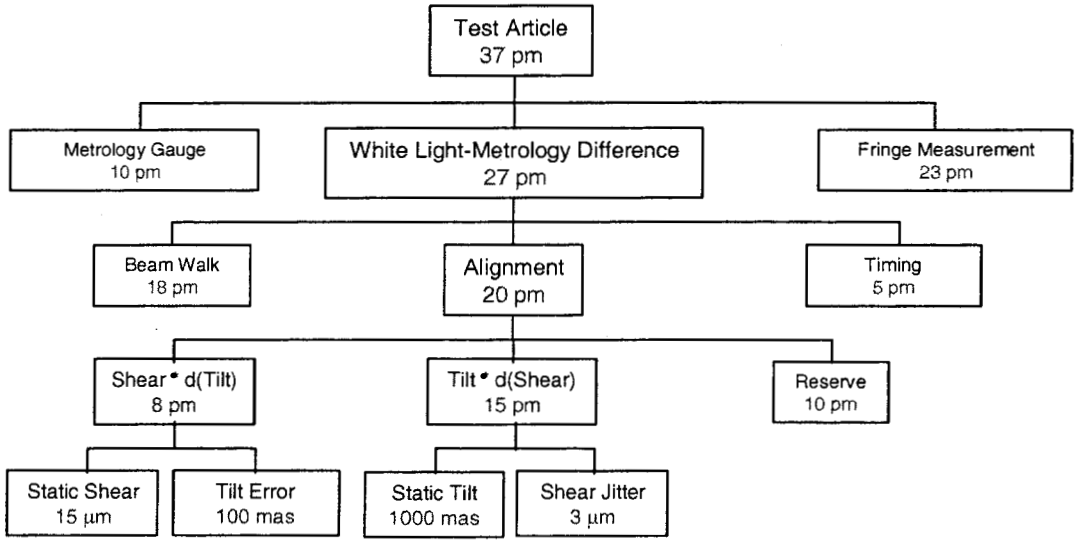

Figure 4: Partial MAM error tree

We have to be concerned about the absolute tilt and shear between the star light beam, the metrology measurement beam and the metrology local oscillator, on both the Pseudo-Star side and the Test-Article side. Indeed there is a dozen of error sources just related to initial alignment. The requirement table (Table 1) shows the detail error allocation for each of them. We are presenting the detail alignment procedures in the next section.

MAM Optical Alignment Term	Static shear (um)	Tilt drift (urad)	Static tilt (urad)	Shear drift (um)	Error (pm)
IIPS, white-light/metrology tip/tilt			10	3	30
IIPS, white-light/metrology shear	7	4			28
IIPS, metrology (Measure/LO) tip/tilt			x	x	xx
IIPS, metrology (Measure/LO) shear	x	x			xx
TA, white-light/metrology tip/tilt			x	x	xx
TA, white-light/metrology shear	x	x			xx
TA, metrology (Measure/LO) tip/tilt			5	3	15
TA, metrology (Measure/LO) shear	15	0.5			7.5
North/South arms, tip/tilt			x	x	xx
North/South arms, beam shear	x	x			xx
TOTAL:					**50**

Table 1: Detail error allocation requirements.

4. SENSORS AND ACTUATORS

4. 1. White light detector: CCD.

The central sensor in MAM is the CCD camera, a small-format (40x40) silicon device used to monitor fringes in the white-light beam as the interferometer OPD is scanned a few wavelengths by the voice-coil modulator (VCM). Owing to the prism disperser that precedes it, the CCD camera has one spatial and one spectral dimension. The spectral dimension covers roughly 600-1000 nm, encompassing the auxiliary HeNe metrology beam at 633 nm or the FAM at 660 nm, and most of the light emitted by the white-light source, a 3100-K blackbody.

4. 2. Metrology detector

Heterodyne detection for metrology is done within the boxes labeled "metrology launcher" in Figure 2. There are two independent launchers on the TA and on the IIPS side of MAM. Each launcher sends out two independent sets of dual measurement beams that traverse the two arms of TA or IIPS, where they are ultimately retro-reflected from the small corner cubes mounted in the sub-aperture of the two siderostats. The roundtrip distance is measured by heterodyne interferometry against a reference beam (local oscillator, or "LO") that is kept physically confined within each launcher. Measurement and reference beams are coherent, but shifted in frequency by a small amount (~40 MHz). The measurement beams are sent out in pairs as square pencil beams, 3.5 mm on a side, within the sub-aperture. The SAVV masks located as shown in Figure 2 ensure that the beams for one arm are arranged side by side horizontally, and for the other are stacked vertically, so there is no confusion between the two heterodyne signals. The final detection for the two arms is made by two distinct photodetectors within the launcher.

4. 3. Alignment quad-cells and shear sensors

A number of sensors have been built into MAM specifically to monitor optical alignment, and a number of actuators have been implemented to make the adjustments to the alignment that are indicated by the readings of the sensors. Sensors generally measure pointing (tip/tilt) or beam shear; these may be accomplished with quadrant detectors ("quad-cells") at a focal plane or at a pupil plane, respectively. MAM uses two kinds of quad-cells: silicon detectors that are sensitive to visible light at wavelengths shorter than about one micron, and InGaAs detectors that are sensitive to the near-infrared (specifically, to 1319 nm metrology radiation) and to wavelengths as short as just below one micron. Formal centroid accuracy is very high, if only photon signal-to-noise ratio is considered, but irregularities in detector properties (e.g. spatial variations in quantum efficiency) limit the accuracy in practice.

Piezo-electric drives (PZTs) are used when smooth, fast motions over relatively short strokes are required, as with the FSMs and the IIPS steering mirrors. The IIPS steering mirrors also have a second stage of motors, Burleigh Inchworms, which are also piezo-electrically driven. Encoded servo-motors from Oriel are used to drive the siderostats and the actuators that translate the pupil mask. Stepper motors are used to drive the interferometer delay line on the Test Article side, and the translation stage that moves the steering mirror towers on the IIPS side. Motorized adjustment screws from New Focus, called "picomotors", are used for a number of remaining functions of a less precise nature that must be actuated in MAM, where repeatability is not an issue. Finally, DC motors are used to insert masks in and out of the beams. All motors must, of course, be vacuum compatible. The PZT-based models, but particularly the Burleigh Inchworms, are susceptible to damage in a certain range of pressures, about 1 to 1000 milli-Torr, the "corona" region, over which these relatively high-voltage devices will arc.

5. ALIGNMENT PROCEDURE

The alignment procedure for MAM is necessarily complex, but there are some simple underlying tactical themes. The vertices of the corner cubes mounted on the sub-apertures of the two siderostats mark the precise dividing line between TA and IIPS (see Figure 7). Alignment of TA metrology and IIPS metrology are independent problems, of course, as each gauge measures roundtrip distances to the vertices from opposite directions. But alignment of the white light used for the interferometer is highly coupled. For white light, alignment generally begins at the light source in IIPS and work down the optical paths toward the sensors in TA. For both white light and metrology, it is generally advantageous to accomplish tip/tilt alignment of two beams first, and then beam shear and/or overlap from the two arms.

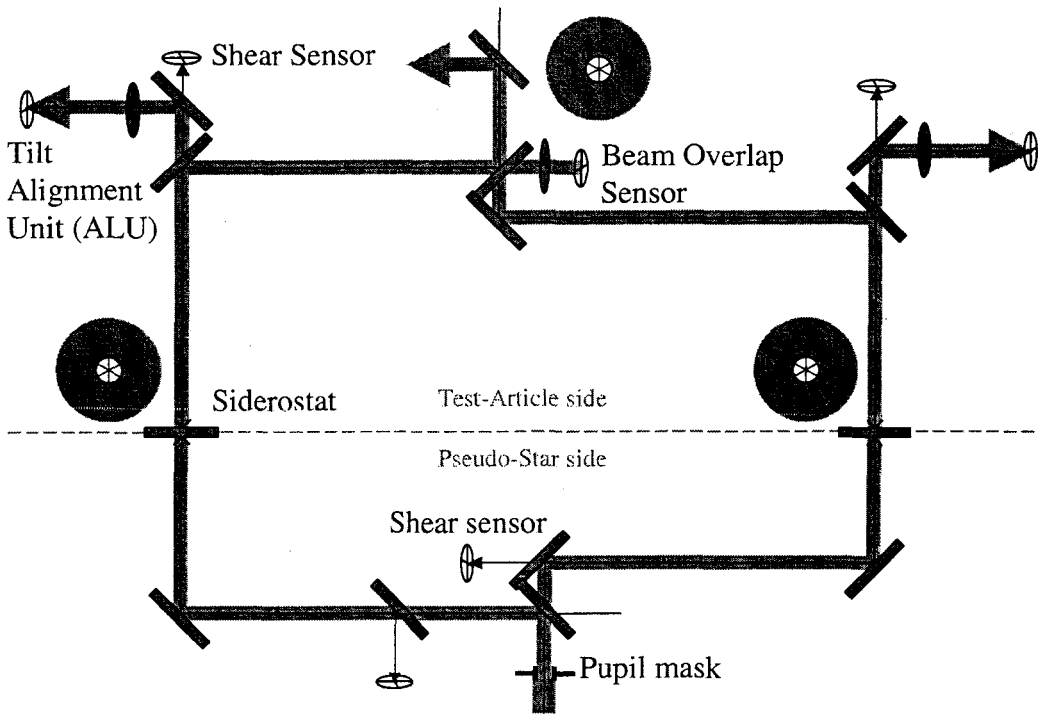

Figure 7: Alignment sensors

While Figure 7 provides a schematic overview, there are many motorized actuators and auxiliary sensors not shown. These include motorized shutters, pupil masks, metrology masks, and quadrant detectors (some also motorized), some configured as tip/tilt sensors and some as beam shear sensors. Some have been briefly described in previous sections.

5. 1. TA (Test Article) metrology

The first step in aligning the 1319 nm metrology beam in TA is an internal adjustment of the metrology gauge itself. The gauge is a heterodyne interferometer that compares a "measurement" beam, which is sent out to traverse a roundtrip through the TA optics, to a "reference" or local oscillator (LO) beam, coherent but slightly shifted in frequency, that remains within the launcher. The two beams pass through an internal set of Risley prisms that have been adjusted to minimize beam shear. A corner cube is then inserted by a motorized actuator in front of the launcher, so the measurement beam is retro-reflected and the relative tip/tilt between it and the internal LO beam may be adjusted with motorized wedges driven by picomotors. A unique feature of the SAVV metrology launcher is that it sends out two independent measurement beams to traverse the two arms of the interferometer, though only a single LO beam is needed. The tip/tilt adjustment is thus done to maximize the metrology signal amplitudes, and to keep the two independent metrology signals in phase, ensuring equal paths within the metrology gauge

Now the motorized corner cube is removed, and the measurement beams are sent out to the two corner cubes mounted in the subapertures of the two siderostats. SAVV masks keep the beams traversing the two arms of the interferometer separate, so two distinct heterodyne signals are produced by two photodetectors within the metrology launcher. The metrology signal amplitude for one arm (the South arm) is maximized by moving the flat mirrors arranged as a periscope in front of the launcher; these are motorized with picomotors. The effect of moving the periscope mirrors is to translate the metrology beam on the siderostat corner cube, and maximum signal should occur when that beam is centered on the corner cube vertex. When the South arm alignment is completed, the metrology signal amplitude for the other (North) arm is maximized by tilting the main beam combiner in TA, which is motorized with picomotors.

Now that the metrology beams have been established on both arms of TA, the infrared shear sensors (quad-cells) are adjusted in transverse position to put one of the dual metrology spots at their centers. Each quad-cell is mounted on a translation stage, driven by picomotors, to simplify this adjustment.

5. 2. IIPS (Pseudo Star) metrology

The operation of the metrology gauge in IIPS, measuring the roundtrip distance from the launcher to the corner cubes mounted in the sub-aperture of the TA siderostats, is very similar to that of the gauge in TA, and the alignment procedures are similar as well. As before, an auxiliary corner cube on an actuated shutter is inserted in the beam immediately in front of the launcher, and wedges motorized with picomotors are used to adjust the tip/tilt between measured and LO beams until a maximum of the heterodyne metrology signal is achieved.

The next alignment step makes use of the so-called "split-SAVV" beam, which is the coherent 1319 nm metrology ("IR") beam launched from the cube beam splitter along with the white light beam in Figure 2. Because it is injected identically, split-SAVV is a useful tracer for white light. This fact is exploited by disconnecting the IR fiber that usually injects LO power into the metrology launcher, and moving it to inject the IR light via the cube beam splitter. The LO-powered split-SAVV beam thus produced will interfere with the two measurement beams sent out in the usual way by the metrology launcher, and produce heterodyne signals for each arm of IIPS. These signals are maximized for each arm by adjusting the tip/tilt of the flat mirrors in the periscope adjacent to the launcher. There are several local maxima in a two-dimensional envelope, but the central maximum, where the two metrology signals are in phase, giving equal paths on the two arms, must be found. When this is accomplished, parallelism will be established between the metrology measurement beam and the white light beam, which the split-SAVV beam has been emulating; the IR fiber is then returned to its standard position, delivering LO power to the metrology launcher.

We next maximize the metrology signal amplitude for the South arm by tilting the IIPS steering mirror on that arm. This will have the effect of translating the metrology beam on the corner cube mounted in the sub-aperture of the TA siderostat, and a maximum return signal will correspond to minimizing the shear of the measurement beam with respect to the corner cube vertex (i.e. centering it). This shear alignment is then repeated for the North arm using the other IIPS steering mirror.

The final adjustment for the IIPS metrology system is moving the shear sensors laterally until the metrology beams are at the null positions of the quad-cells. These shear sensors are also motorized, with picomotor-driven translation stages. Since the shear sensor quad-cell will define the reference position to keep the alignment while the artificial star is articulated through the narrow angle field of view (1 degree), it is critical to properly adjust their position.

5. 3. Starlight/Metrology parallelism

Parallelism alignment between metrology light and white light was accomplished on the IIPS side of the experiment as part of the metrology alignment of the previous section. On the TA side, this alignment is carried out with the Alignment Unit (ALU). On each arm, the ALU feed mirror is adjusted to put the TA metrology spots on the IR quad-cells at the null positions. Then, again independently on each arm, the 532 nm green laser beacon is used as a tracer for the white light beam, and is brought to the null position of the corresponding visible-light ALU quad-cell by moving the siderostat on that arm. It is now possible to servo the fast-steering mirrors (FSMs) on each arm using drive signals derived from the green laser beacon on the appropriate ALU visible-light quad-cell.

5. 4. Pointing loop reference

For this alignment, the FSM pointing loops must be kept closed on the initial targets that were set during the TA alignment described in the previous section. (Large steady-state deflections of the FSMs as the system drifts must be offloaded to the siderostats, to avoid shear of the metrology beams on the siderostat corner cubes.) In addition to the green laser beacon, the HeNe laser that is injected with the white light source via the cube beam splitter in IIPS is turned on. The HeNe beam will form a spot on the CCD in TA, and picomotor-driven translation stages are used to center that spot on the target location that gives the correct shift to image the entire spectral range needed by MAM. If the interferometer OPD is scanned by the voice coil modulator (VCM), the HeNe spot will vary in intensity and a fringe visibility may be derived. This visibility is maximized by adjusting the offset of the North-arm FSM, within the feedback loop that is kept closed. When this is done, the final pointing target that will maintain high-visibility fringes has been established.

5. 5. Starlight/Metrology overlap in shear (the "pointing decenter" test)

There is no easy way to directly adjust the white light and metrology beam shear, as device variations over the face of a quad-cell limit the practical precision to which the center of a large-diameter beam defining a pupil may be found. However, we may use the OPD signature from the interferometer itself, discussed in section 3 and diagrammed in Figure 3, that arises when beams with differential shear undergo pointing changes. As applied to MAM, this technique is called the "pointing decenter" test. We articulate TA white-light pointing with the FSMs, but this has no effect on the sub-aperture metrology beams, and so a variation in the tip/tilt angle $\Delta\varphi$ between the two beams is introduced. This will multiply the shear offset S, that we seek to measure, to produce a recognizable variation in OPD between white light and metrology, Δd, that is given by $\Delta d = S \cdot \Delta\varphi$ (see Figure 3).

For the pointing decenter test, the voice-coil modulator (VCM) is run at 20 Hz with a triangle wave of 2 μm stroke, to permit the basic fringe-fitting that is needed to monitor white-light OPD. At the same time, the FSM in the arm for which white-light and metrology beams are being shear-aligned is run with a slow sinusoidal tip/tilt modulation, with an amplitude of about 1 μrad. The CCD, metrology gauges, and pointing quad-cells are run at 500 Hz. A typical measurement run takes 5 minutes. The shear offset thus derived ($S = \Delta d / \Delta\varphi$) is corrected by moving the pupil mask, which defines the photocenter of the white-light beam. Measurements and pupil mask shifts are iterated until white light and metrology beams are brought into shear alignment to the desired accuracy.

6. RESULTS

A useful tool for expressing the performance of MAM is the Allan variance of the difference between OPD measured by the white-light interferometer and OPD measured by the metrology gauge. Roughly speaking, the Allan variance (or its square root, the Allan deviation) assesses the mean-square error in the OPD difference as a function of the time interval over which the data are averaged. It takes into account the temporal structure of the noise, which SIM will also do by interleaving multiple chopped observations of target and calibration stars. Allan variance plots also have diagnostic value, as many common noise mechanics have characteristic power-law signatures. Our definition takes one-half the mean square of the differences between successive averaging bins of duration t, and this quantity is plotted against t. For any given astrometric performance level required of SIM, an equivalent performance level for MAM, in picometers of OPD difference, may be derived. So the progression of the MAM experiment has been to push the noise minimum to ever lower levels, in picometers, and to make sure that is occurs on a time-scale suitable for realistic SIM chopping cycles.

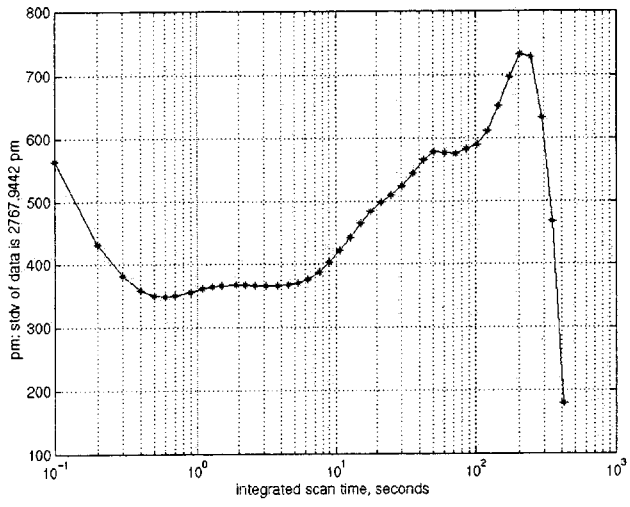

Figure 8: RT Allan variance prior to precision alignment

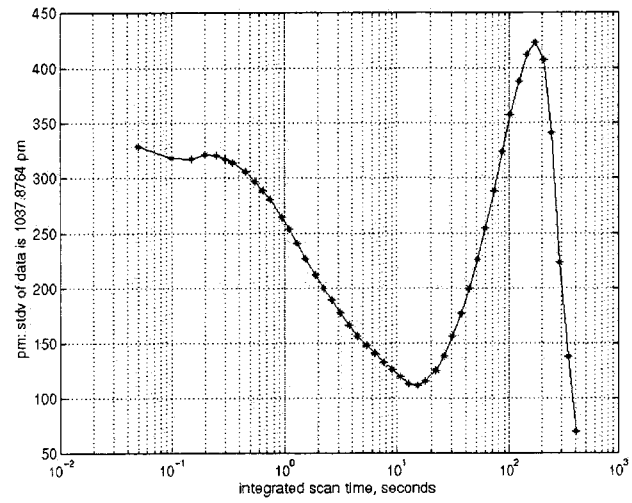

Figure 9: RT Allan variance after the precision alignment

In Figure 8, we show a modified Allan variance plots for MAM. This represents the performance of the system with coarse alignment only. To calculate this pseudo-Allen variant, the data are cut in successive portions of same duration. The vertical axis is the standard deviation of the average value for each successive portion (with the linear drift removed). The horizontal axis is the length in time of each portion (integration time). The first point is the standard deviation of the raw data. The last point is zero (standard deviation of only two portions with the linear drift removed).

At short period (0.1s to 1s), the performance is limited by random noise, such as vibration, electronic and photon noise. At long period (10s to 100s), the performance is limited by thermal drifts. After 200s, the data should be ignored because of the lack of samples for the standard deviation. The best performance (350pm) is reached in about 0.5s, and after a few seconds the performance decreases because of the lack of precision alignment.

Figure 9 shows the performance obtained after the precision alignment described in the paper. At short period (0.1s to 10s), the performance keeps on improving with the integration time until we reach the 120pm minimum in about 15s. The drift is still present at longer integration time, but the amplitude is much smaller. At 100s, the performance is still below 350pm. These data suggest an optimum integration time of 15 seconds.

7. CONCLUSION

We have discussed some of the critical errors incurred by the MAM testbed for SIM that arise from slight misalignments of the optics, and have presented a systematic procedure for bringing them into the range required by MAM's error budget. Recent static data taken with the MAM testbed have validated the alignment approach. The alignment scheme for the SIM will inherit from our experience. We are planning additional tests to optimize the sequence and assess the performance of the system in the narrow-angle field of view.

ACKNOWLEDGMENTS

The research described in this publication was performed at the Jet Propulsion Laboratory of the California Institute of Technology, under contract with the National Aeronautics and Space Administration. The results presented are the fruits of an entire team. The authors would like to thank in particular: Dennis Lapicz and Robert Irigoyen for setting up all the sensors and for helping in the laborious alignment.

BIBLIOGRAPHY

1. J. Marr, "Space Interferometry Mission (SIM) overview and current status," *SPIE conference Interferometry in Space*, vol. 4852, 2002.

2. B. E. Hines, C. E. Bell, R. Goullioud, R. Spero, G. W. Neat, T. J. Shen, and E. E. Bloemhof, "Micro-arcsecond metrology (MAM) testbed overview," *SPIE conference Interferometry in Space*, vol. 4852, 2002.
3. R. P. Korechoff, "MAM beam walk sensitivities," JPL Interoffice Memo, Dec. 10, 2001.
4. D. B. Schaechter, P. Perkins, C. Tischhauser, D. A. Swanson, R. S. Benson, T. B. Andersen, P. V. Mammini, "Diffraction testbed and results," *SPIE conference Interferometry in Space*, vol. 4852, 2002.
5. F. Zhao, R. Diaz, G. M. Kuan, N. Sigrist, Y. Beregovski, L. L. Ames, K. Dutta, "Internal metrology beam launcher development for the space interferometry mission," *SPIE conference Interferometry in Space*, vol. 4852, 2002.